ARTICLE

Electrocatalytic Oxidation of Saccharides at MoO_x/AuNPs Modified Electrode Towards Analytical Application

Shou-guo Wu*, Zhi-xin Zhang, Qi-ping Zhao, Lei Zhou, Yao Yao

Department of Chemistry, University of Science and Technology of China, Hefei 230026, China

(Dated: Received on May 7, 2014; Accepted on June 3, 2014)

The MoO_x/AuNPs composite film modified glassy carbon electrode was fabricated by electro-depositing simultaneously gold nanoparticles and molybdenum oxides using cyclic voltammetry. The morphology and topography of the MoO_x/AuNPs composite were characterized by scan electron microscopy and X-ray photoelectron spectroscopy respectively, and the electrocatalytic oxidation of glucose at the MoO_x/AuNPs composite film was investigated and analyzed in detail. It was shown that the MoO_x/AuNPs composite was of strong electrocatalytic activity towards oxidation of glucose as well as other saccharides, so that an attempt was made for direct voltammetric determination of glucose. Then the positive scan polarization reverse catalytic voltammetry was proposed for the first time. Based on this method, the pure oxidation current was extracted by subtraction of the blank current in the reverse scan. The current sensitivity was enhanced tremendously and the signal to noise ratio was improved adequately. The electrocatalytic oxidation of glucose at the MoO_x/AuNPs modified electrode was performed in alkaline medium, a wide linear range from 0.01 mmol/L to 4.0 mmol/L of glucose, a higher current sensitivity of 2.35 mA/(mmol/L·cm^2), and a lower limit of detection of 9.01 μmol/L (at signal/noise=3) were achieved. In addition, the electrocatalytic oxidation of other saccharides such as lactose, fructose and sucrose was also evaluated.

Key words: Molybdenum oxide, Gold nanoparticle, Non-enzymatic biosensor, Positive scan polarization reverse catalytic voltammetry

I. INTRODUCTION

Highly sensitive detection toward glucose is very desirable due to its widespread application in the fields of clinical chemistry, biochemistry, environmental, glucose-oxygen fuel cells, and food chemistry [1−4]. The sensing of saccharides finds widespread exploitation in analytical and forensic applications [5]. Since the first glucose sensing platform was reported by Clark and Lyons [6], glucose oxidase (GO) based and glucose dehydrogenase (GDH) based glucose sensing platform have been widely used in the detection of blood glucose [7−10]. However, a number of critical drawbacks hinder its further development. In view of the nature of the enzymes, the most common and serious problem concerning the enzymatic glucose sensing platforms lies in their rigorous operational conditions (such as solution acidity, temperature, *etc.*) and the intrinsic instability. In addition, the use of expensive enzyme is also unfavorable in term of cost-effectiveness. In the hope of improving the electrocatalytic activity and selectivity towards the oxidation of glucose, many non-enzymatic glucose sensing platforms have also been explored [11−14].

Direct non-enzymatic electrocatalytic oxidation of glucose varies considerably depending on the electrode material used, such as transition metal nanomaterials, nanostructured metal oxides and complexes, alloy nanomaterials and carbon based materials [15−18]. Among these materials, precious metals such as gold, platinum, palladium and transition metals including copper and nickel are well known to be good electrocatalysts due to their ability to adopt multiple oxidation states and adsorb other species on their surfaces to form intermediates. Recently, much attention has been paid to Au nanomaterials modified electrodes such as Au nanowire [19], nanoporous Au [20], and Au nanotube [21], because of their highly catalytic activity for glucose oxidation.

Enhancement of electrocatalytic activity of gold electrodes is usually actualized by dispersing gold into small or even nano-scale sized metal oxide particles or alloying gold with other metals. Many heterogeneous metal based electrodes were widely studied because they have the same high electro-conductivity as carbon materials such as carbon nanotube and graphene. In contrast to noble metal based electrodes, the heterogeneous metal based electrodes show an excellent electrocatalytic activity for glucose oxidation without observable self-pois

*Author to whom correspondence should be addressed. E-mail: sgwu@ustc.edu.cn

oning. Recently various attempts have been made and modified electrodes made from NiO/Au [22], Nano Au/TiO_2 [23], $Au/Ni(OH)_2$ [24], and Au/MnO_2 [25] were widely investigated.

It has been demonstrated that MoO_x has good electro-catalytic properties for oxidation of different organic molecules. For example, molybdenum oxide modified electrode was reported to detect iodate in salt samples [26]. Çakar *et al.* investigated the monitoring of oxygen consumption using glucose oxidase (GO) as the model enzyme on a glassy carbon electrode modified with platinum and molybdenum oxide (Pt/MoO_x) [27].

In this work, a new type of electrocatalytic platform for glucose oxidation based on MoO_x/AuNPs composite film was prepared by cyclic voltammetric deposition process in order to find a convenient non-enzymatic electrode for direct determination of glucose and other saccharides with voltammetry.

II. EXPERIMENTS

A. Reagents and apparatus

$NaMoO_4$, $HAuCl_4$, Na_2SO_4, H_2SO_4, NaOH, and glucose were analytical grade and were all purchased from Shanghai Chemical Reagent Company (Shanghai, China) and used without further purification. All electrochemical experiments were carried out on a LK2005 electrochemical work station (LANLIKE, Tianjing, China). The three-electrode system consisted of a MoO_x/AuNPs modified glass carbon electrode (GCE, 3 mm in diameter) as working electrode, a reference electrode (saturated calomel electrode), and a counter electrode (platinum wire). Cyclic voltammetry was employed for preparation of the modified electrodes and voltammetric determination of analytes. All experiments were performed at room temperature, and high purity nitrogen was used to de-aerate the solution if necessary. Scanning electron microscope (SEM) images were obtained on a JEOL JSM-6700F SEM system. X-ray photoelectron spectroscopy (XPS) measurements were performed on an ESCALAB MK2 spectrometer (VG Co., UK) with Mg Kα radiation as the excitation source.

B. Preparation of AuNPs, MoO_x, and MoO_x/AuNPs modified GCE

The GCE was polished on a piece of faux suede cloth with alumina slurry and then rinsed with pure water. After that it was placed into a beaker containing deionized water in an ultrasonic bath for 5 min. The MoO_x, AuNPs, and MoO_x/AuNPs films were electrodeposited on GCE respectively in different electrolytes with cyclic voltammetry in the potential range of -0.8 V to 0.3 V at 50 mV/s for 5 cycles. For MoO_x film, it was in 0.5 mmol/L $NaMoO_4$, 50 mmol/L Na_2SO_4 and 18.4 mmol/L H_2SO_4 aqueous solution, for AuNPs film it was in 10 mmol/L $HAuCl_4$ and 18.4 mmol/L H_2SO_4 aqueous solution, and for MoO_x/AuNPs film it was in 10 mmol/L $HAuCl_4$, 0.5 mmol/L $NaMoO_4$, 50 mmol/L Na_2SO_4 and 18.4 mmol/L H_2SO_4 aqueous solution.

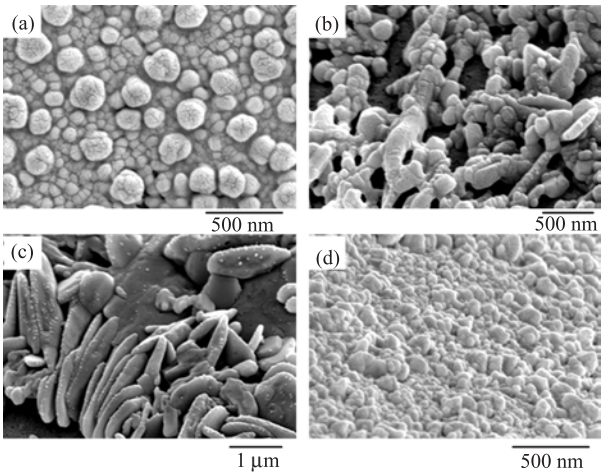

FIG. 1 SEM images of different modified electrodes. (a) AuNPs/GCE, (b) and (c) MoO_x/GCE, (d) MoO_x/AuNPs/GCE.

C. Determination of glucose using the positive scan polarization reverse catalytic voltammetry

A novel method, the positive scan polarization reverse catalytic voltammetry (PSPRCV), was developed based on cyclic voltammetry for determination of glucose. For PSPRCV, like cyclic voltammetry, the potential is firstly scanning positively from initial (-0.8 V) to switching potential (+0.6 V), the working electrode is anodic polarized, then the potential is scanning reversely (negatively) to the initial, meanwhile the glucose will be catalytic oxidized by the electrode reaction intermediate products, and the voltammogram is recorded. Finally, the blank data (without glucose) is deducted from the sample data (with glucose). The difference value peak current is proportional to the bulk concentration of glucose.

III. RESULTS AND DISCUSSION

A. Characterization of the MoO_x/AuNPs composite film

The SEM images of morphologies and crystal phase structures of the prepared AuNPs, MoO_x and MoO_x/AuNPs thin films electrodeposited on GCE are shown in Fig.1. The pure AuNPs sample (Fig.1(a)) consists of nanoparticles with the diameter range from $\sim$20 nm to 200 nm, and the surface of the nanoparticles were cracked which increased the surface area efficiently. Note that this surface topography was critical since it

DOI:10.1063/1674-0068/27/05/600-606

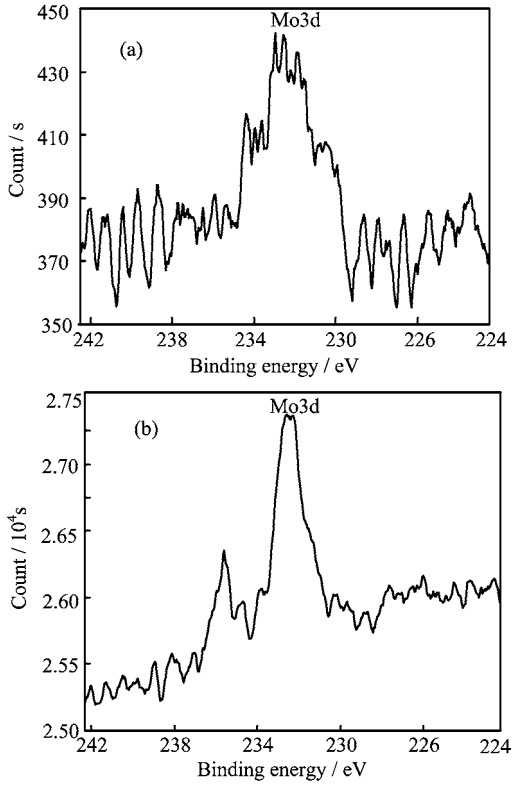

FIG. 2 XPS spectra of Mo3d scan chart of (a) MoO_x and (b) MoO_x/AuNPs.

improved the adsorption capability for small molecules and defined the inherent reproducibility and electrochemical performance of the platform. The MoO_x sample (Fig.1 (b) and (c)) shows a combination of spherical and cake-like sediments resembling that of two different crystal structures which indicated that the MoO_x film could be a composite of MoO_2 and MoO_3. However, the co-electrodeposited MoO_x/AuNPs showed a completely different surface topography compared to MoO_x and AuNPs (Fig.1(d)). It was revealed there were some effect forces between molybdenum oxides and gold nanoparticles, as a result, the mixed irregular nanoparticles formed in the range of 40−100 nm which was finer and tighter than MoO_x and AuNPs. It means that MoO_x/AuNPs composite film may possess synergistic effect to enhance its electrocatalytic activity.

XPS is a powerful technique for the study of transition metal compounds having localized valence-orbitals. The MoO_x and MoO_x/AuNPs thin films were further characterized by XPS as shown in Fig.2. In the Mo3d region, the band showed a single peak at 232.95 eV corresponding to the $3d_{2/5}$ spin system of MoO_x. Whereas the corresponding peaks for the MoO_x/AuNPs film appears spin system of Mo $3d_{2/5}$ at 232.6 eV (Fig.2(b)), and that the peak strength was about twenty-five times higher than that in MoO_x, so much higher binding energy illustrates a strong interaction existing between Au and Mo, which may be combined by an alloyed intermetallic compound.

B. Electrocatalytic behavior of the MoO_x/AuNPs towards glucose oxidation

The electrochemical behavior of MoO_x, AuNPs, and MoO_x/AuNPs film modified GCE was studied by cyclic voltammetry in alkaline electrolyte solution. Figure 3 shows the cyclic voltammograms in absence and presence of 5 mmol/L glucose in 0.10 mol/L NaOH solution at the AuNPs modified GCE, the MoO_x modified GCE, and the MoO_x/AuNPs composite modified GCE.

It was shown from Fig.3(A), in absence of glucose, there was two pairs of redox peaks at the AuNPs modified electrode in alkaline solution (curve a). In the positive scan, Au was oxidized consecutively from Au(0) to Au(I), then to Au(III), which was subsequently reduced back from Au(III) to Au(I), then to Au(0) in the reversal scan. Two anodic peaks at −0.08 and 0.45 V can be assigned to the oxidation of Au(0) to Au(I) and Au(I) to Au(III), respectively. And two cathodic peaks at +0.16 and −0.18 V can be considered as the reduction of Au(III) to Au(I) and Au(I) to Au(0), respectively. In presence of glucose (curve b), two oxidation peak potentials of Au were shifted negatively from −0.08 V to −0.38 V and 0.45 V to 0.20 V respectively, and the peak currents were increased tremendously. This is ascribed to the strong catalytic activity of the intermediate product Au(I) towards glucose oxidation. Similarly, in the reverse scan, due to generation of Au(I) from the reduction of Au(III), a strong oxidation peak of glucose was observed at around 0.05 V. The electrocatalytic mechanism could be described as follows.

In the positive scan:

$$\mathrm{Au} \rightarrow \mathrm{Au(I)} + \mathrm{e}^- \quad (-0.38\ \mathrm{V})\ (1)$$

$$\mathrm{Au(I)} + \mathrm{glucose} \rightarrow \mathrm{Au} + \mathrm{glucose\ acid} \quad (+0.20\ \mathrm{V})\ (2)$$

$$\mathrm{Au(I)} \rightarrow \mathrm{Au(III)} + \mathrm{e}^- \quad (+0.45\ \mathrm{V})\ (3)$$

In the reverse scan:

$$\mathrm{Au(III)} + \mathrm{e}^- \rightarrow \mathrm{Au(I)} \quad (+0.16\ \mathrm{V})\ (4)$$

$$\mathrm{Au(I)} + \mathrm{glucose} \rightarrow \mathrm{Au} + \mathrm{glucose\ acid} \quad (+0.05\ \mathrm{V})\ (5)$$

$$\mathrm{Au(I)} + \mathrm{e}^- \rightarrow \mathrm{Au} \quad (-0.18\ \mathrm{V})\ (6)$$

Reaction (2) makes the oxidation reactions (1) and (3) easier, resulting in the peak potentials shifting negatively and the peak currents increased remarkably. Oppositely, due to reaction (5), the reduction peaks of reaction (4) and (6) almost disappeared, instead, a strong oxidation peak corresponding to reaction (5) appeared.

At the MoO_x modified GCE (Fig.3(B)), the redox peaks were very weak (curve c), and had slight change with the addition of glucose (curve d) because of the limited catalytic capability of MoO_x.

The cyclic voltammograms at the MoO_x/AuNPs modified GCE are demonstrated in Fig.3(C). Although

DOI:10.1063/1674-0068/27/05/600-606

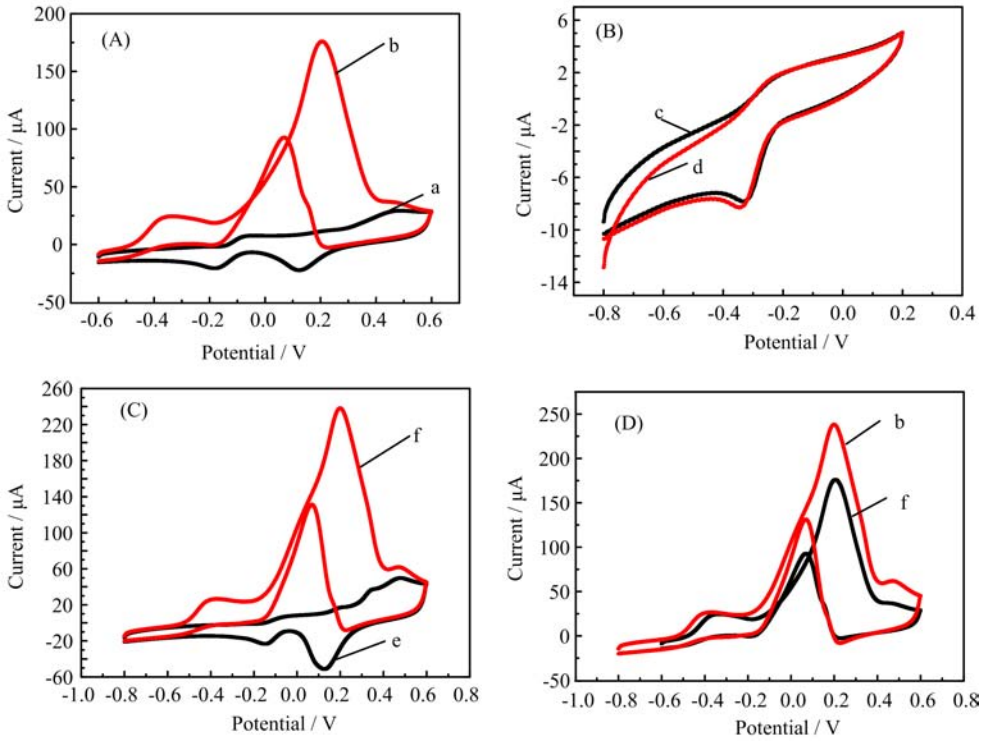

FIG. 3 Cyclic voltammograms at (A) AuNPs, (B) MoO_x, and (C) MoO_x/AuNPs modified GCE in absence (a, c, e) and presence (b, d, f) of 5 mmol/L glucose in 0.10 mol/L NaOH solution. (D) Comparison of the cyclic voltammograms of the AuNPs and the MoO_x/AuNPs modified GCE in presence of 5 mmol/L glucose. Scan rate: 100 mV/s.

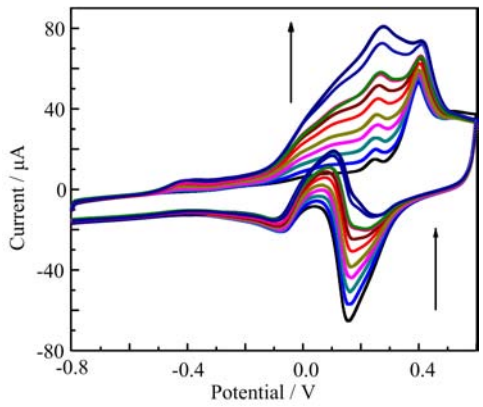

FIG. 4 The cyclic voltammograms in different concentrations of glucose. From bottom to top: 0, 0.1, 0.2, 0.3, 0.4, 0.5, 0.6, 0.7, 0.8, 0.9, and 1.0 mmol/L.

the gold reaction mechanism is similar to the AuNPs modified GCE, due to the doping of molybdenum oxides, there appeared two weak peaks in the positive scan at ca. 0.2 and 0.35 V respectively, resulting from the oxidation of molybdenum from lower valence state to higher state (Fig.3(C), curve e). In the reverse scan, the reduction peak current was enhanced due to existence of the intermediate products of molybdenum oxides. So that, with the addition of glucose, the catalytic oxidation peak currents of glucose were increased ca. 40% both in the positive and reverse scans (Fig.3(D)). It was indicated clearly, for MoO_x/AuNPs composite, there was a synergetic effect on the catalytic oxidation of glucose.

The oxidation current of glucose both in the positive and reverse scan, was dependant on the bulk concentration of glucose, the peak currents were increased with the concentration increasing. Figure 4 gives the cyclic voltammograms of the MoO_x/AuNPs modified GCE in different concentrations of glucose solution. It can be seen from Fig.4, in the reverse scan, when the concentration of glucose was lower, the reduction peak current (corresponding to reaction (4)) was decreased gradually with the concentration increasing, meanwhile the oxidation peak current (corresponding to reaction (5)) was increased steadily.

C. Analytical performance of the MoO_x/AuNPs towards glucose detection

Although the oxidation peak current both in the positive and reverse scan increased with the concentration of glucose increasing, the oxidation peak in the positive scan (corresponding to reaction (2)) is complex and poor reproducible because it was completely overlapped with the oxidation of molybdenum oxides as well as with that of Au(I) (corresponding to reaction (3)), so it was not suited for the quantitative detection of

DOI:10.1063/1674-0068/27/05/600-606

TABLE I Comparison of performances of various glucose sensing platform.

Electrode composition	Sensitivity[a]	Linear range/(mmol/L)	LOD/(μmol/L)	Reference
Au nanowire array	0.04	0.1−20	0.003	[28]
Au NPs/Indium tin oxide	0.1835	0.004−0.5		[29]
Cu NPs/MWCNTs	0.714	0.01−0.3	0.5	[30]
Mn_3O_4/3D graphene	0.36	0.1−8	10	[16]
Pd/CuO nanofibers	1.061	0.2−2.5	0.019	[32]
MnO_2/AuNPs composite	0.096	0.1−20	1	[25]
Pt/MoO_x/GCE/GO		0.05−0.5	25	[27]
MoO_x/AuNPs	2.35	0.01−4	9.01	This work

[a] Sensitivity is in unit of mA/(mmol/L·cm^2).

glucose. The oxidation peak in the reverse scan was simple and well reproducible, and can be used to detect glucose quantitatively. Here, in order to obtain pure oxidation current, the cyclic scan polarization reverse catalytic voltammetry is proposed. In the reverse scan, in absence of glucose, the current is cathodic, which is considered as the blank current. While in presence of glucose, the current is net current consisting of the reduction current of the modified layer and the catalytic oxidation current of glucose, from which the blank current is subtracted, the pure oxidation current of glucose is achieved.

The difference value voltammograms of PSPRCV in different concentrations of glucose are shown in Fig.5(a). Figure 5(b) shows the original voltammograms in the reverse scan. Clearly, the resulting pure catalytic oxidation peak of glucose was a well defined symmetrical peak, and the potential was almost unchanged with the varying concentration of glucose, and the peak current was in direct proportion to the glucose concentration. Figure 5 (c) and (f) show the linear responses in two different concentration ranges, from 0.1 mmol/L to 1.0 mmol/L and 0.01 mmol/L to 0.1 mmol/L, respectively. When the glucose concentration was beyond 4.0 mmol/L, the peak shape would become wide and flatheaded, indicating the maximum catalytic current was achieved. Two linear regression equations were i=2.55+166.29c (0.01−0.1 mmol/L) with a relative coefficient of 0.9972, and i=4.41+67.97c (0.1−1.0 mmol/L) with a relative coefficient of 0.9974, respectively. According to the signal/noise=3, a lower limit of detection (LOD) was calculated to be 9.01 μmol/L. Based on the experimental results, the current sensitivity of the MoO_x/AuNPs composite film modified electrode is estimated to be 2.35 mA/(mmol/L·cm^2) which is much larger than that of any non-enzymatic biosensors. As a biosensor, the performance of the MoO_x/AuNPs modified electrode is compared with those of other reported transition metal nanomaterials, nanostructured metal oxides, metal heterogeneous based complexes, AuNPs and MoO_x based non-enzymatic platform (Table I).

The reproducibility and the stability of the MoO_x/AuNPs composite film were also investigated. The response peak current of the MoO_x/AuNPs modified GCE remained 91% of the initial value after 100 cycles of CV scan in 0.10 mol/L NaOH solution containing 0.5 mmol/L glucose at 100 mV/s. In contrast, the AuNPs modified GCE only remained 85% of the initial value after 10 cycles scan. Six different MoO_x/AuNPs modified GCEs were prepared in same conditions, and used in the same solution containing 0.5 mmol/L glucose. For measurement of peak currents, the relative standard deviation was calculated to be only 2.5%. These results exhibit that the MoO_x/AuNPs modified GCE has a high stability as well as good reproducibility that makes it possible for practical applications.

D. Electrocatalytic oxidation of other saccharides

Figure 6 depicts the PSPRCV difference value voltammograms obtained at the MoO_x/AuNPs modified GCE in different solutions of 0.010 mol/L NaOH containing lactose, glucose, fructose, and sucrose respectively. Significant voltammetric responses were observed for all saccharide compounds at almost the same peak potential, this is because they possess similar aldehyde base functional groups. Since the sucrose is a non-reducing sugar which contained no anomeric hydroxyl groups, it had the weakest response. For fructose, the free ketone groups can isomerizate to aldoses in alkaline solution, which indicated the similar oxidation activity with glucose. For lactose, which was a disaccharide derived from the condensation of galactose and glucose, had more active aldehyde groups than glucose and fructose, and was more sensitive to the electrocatalytic action of the MoO_x/AuNPs composite. It was shown, as an electrocatalyst, that the MoO_x/AuNPs composite had no selectivity for any single saccharide compound.

IV. CONCLUSION

The MoO_x/AuNPs composite film was successfully synthesized on GCE for the first time by coelectrode-

DOI:10.1063/1674-0068/27/05/600-606

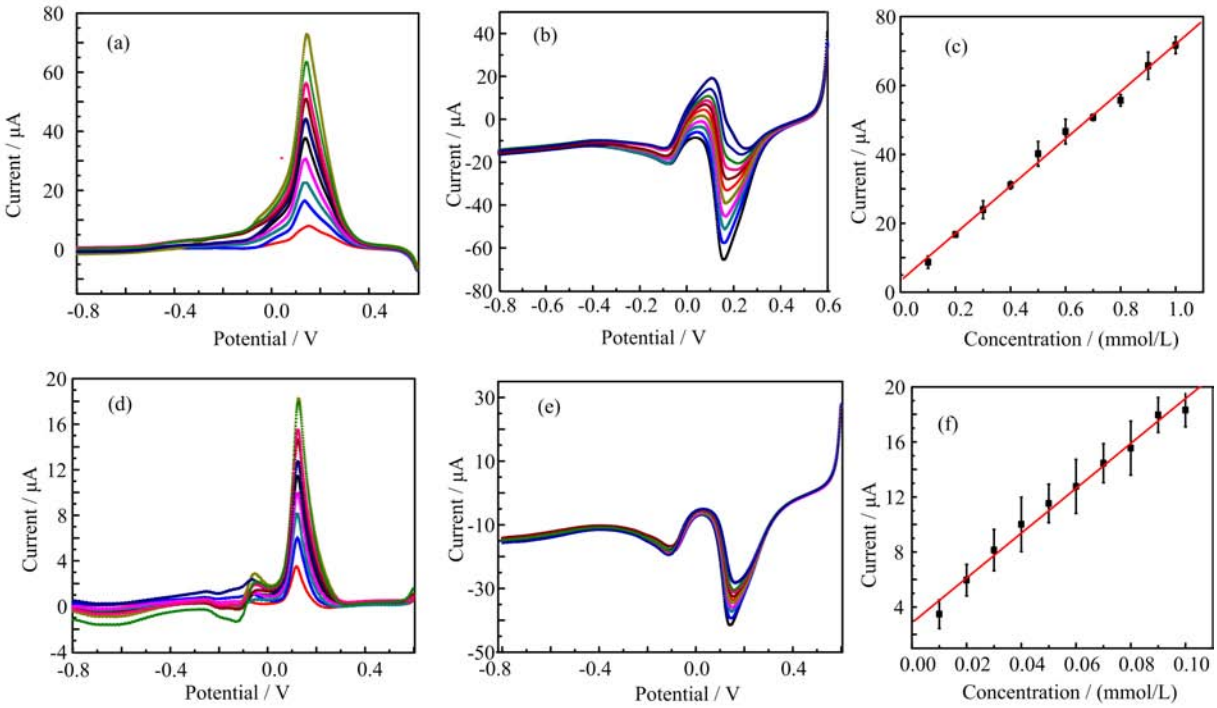

FIG. 5 (a) The PSPRCV difference value voltammograms in different concentrations of glucose solution and (b) original voltammograms in the reverse scan, from bottom to top: 0, 0.1, 0.2, 0.3, 0.4, 0.5, 0.6, 0.7, 0.8, 0.9 and 1.0 mmol/L. (c) The calibration curve of the peak current versus glucose concentration corresponding to (a). (d) The difference value voltammograms of PSPRCV in different concentrations of glucose solution and (e) the original voltammograms in the reverse scan, from bottom to top: 0, 0.01, 0.02, 0.03, 0.04, 0.05, 0.06, 0.07, 0.08, 0.09, and 0.1 mmol/L. (f) The calibration curve of the peak current versus glucose concentration corresponding to (d).

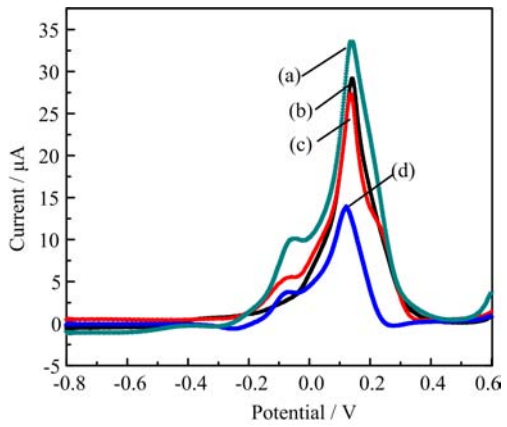

FIG. 6 The PSPRCV difference value voltammograms of saccharides at the MoO_x/AuNPs modified GCE in different solutions of 0.01 mol/L NaOH and 50 mmol/L Na_2SO_4 containing (a) 0.5 mmol/L lactose, (b) 0.5 mmol/L glucose, (c) 0.5 mmol/L fructose, and (d) 0.5 mmol/L sucrose, respectively.

position of gold nanoparticles and molybdenum oxides using cyclic voltammetric method. The MoO_x/AuNPs composite showed higher electrocatalytic activity towards saccharides oxidation in alkaline solution, so that an attempt was made to fabricate the non-enzymatic glucose sensing platform, indicating its potential ability for preparation of the non-enzymatic biosensor. The positive scan polarization reverse catalytic voltammetry was proposed for determination of glucose with higher sensitivity and lower LOD. The difference value current peak of glucose was of a well defined symmetric shape, which was easy to be measured and improved effectively the signal to noise ratio. The major problem was that the MoO_x/AuNPs composite has no selectiveness for catalytic oxidation of glucose due to similar aldehyde groups of the saccharides. Here, it should be stressed that the positive scan polarization reverse catalytic voltammetry will become a brand new and useful method for analysis of catalytic current, and the experiments showed that PSPRCV could not be replaced by the anodic polarization then cathodic scan method, like cathodic stripping voltammetry.

V. ACKNOWLEDGMENTS

This work was supported by the National Basic Research Program of China (No.2013CB933900).

[1] J. Wang, Chem. Rev. **108**, 814 (2008).
[2] L. M. Lu, X. B. Zhang, G. L. Shen, and R. Q. Yu, Anal. Chim. Acta **715**, 99 (2012).

DOI:10.1063/1674-0068/27/05/600-606

[3] J. Lin, C. He, Y. Zhao, and S. Zhang, Sens. Actuat. B **137**, 768 (2009).
[4] M. Tominaga, Y. Taema, and I. Taniguchi, J. Electroanal. Chem. **624**, 1 (2008).
[5] T. J. O'Shea, S. M. Lunte, and W. R. LaCourse, Anal. Chem. **65**, 948 (1993).
[6] L. C. Clark and C. Lyons, Ann. New York Acad. Sci. **102**, 29 (1962).
[7] X. Kang, Z. Mai, X. Zou, P. Cai, and J. Mo, Anal. Biochem. **369**, 71 (2007).
[8] S. G. Wang, Q. Zhang, R. Wang, S. F. Yoon, J. Ahn, D. J. Yang, J. Z. Tian, and J. Q. Li, Q. Zhou, Electrochem. Commun. **5**, 800 (2003).
[9] H. Tang, J. H. Chen, S. Z. Yao, L. H. Nie, G. H. Deng, and Y. F. Kuang, Anal. Biochem. **331**, 89 (2004).
[10] X. Chu, D. X. Duan, G. L. Shen, and R. Q. Yu, Talanta **71**, 2040 (2007).
[11] L. Q. Rong, C. Yang, Q. Y. Qian, and X. H. Xia, Talanta **72**, 819 (2007).
[12] J. Chen, W. D. Zhang, and J. S. Ye, Electrochem. Commun. **10**, 1268 (2008).
[13] W. D. Zhang, J. Chen, L. C. Jiang, Y. X. Yu, and J. Q. Zhang, Microchim. Acta **168**, 259 (2010).
[14] L. Qian, J. Mao, X. Tian, H. Yuan, and D. Xiao, Sens. Actuat. B **176**, 952 (2013).
[15] Z. X. Cao, Y. J. Zou, C. L. Xiang, L. X. Sun, and F. Xu, Anal. Lett. **40**, 2116 (2007).
[16] P. Si, X. C. Dong, P. Chen, and D. H. Kim, J. Mater. Chem. B **1**, 110 (2013).
[17] H. Gao, F. Xiao, C. B. Ching, and H. Duan, ACS Appl. Mater. Interf. **3**, 3049 (2011).
[18] M. Mallesha, R. Manjunatha, G. S. Suresh, J. S. Melo, S. F. D. Souza, and T. V. Venkatesha, J. Solid State Electrochem. **16**, 2675 (2012).
[19] S. Cherevko and C. H. Chung, Sens. Actuat. B **142**, 216 (2009).
[20] S. Cho and C. Kang, Electroanalysis **19**, 2315 (2007).
[21] Y. G. Zhou, S. Yang, Q. Y. Qian, and X. H. Xia, Electrochem. Commun. **11**, 216 (2009).
[22] Y. Ding, Y. Liu, J. Parisi, L. Zhang, and Y. Lei, Biosens. Bioelectron. **28**, 393 (2011).
[23] Q. Yi, W. Yu, Microchimica Acta **165**, 381 (2009).
[24] I. G. Casella, M. R. Guascito, and T. R. I. Cataldi, Anal. Chim. Acta **398**, 153 (1999).
[25] Y. J. Yang and S. Hu, Electrochim. Acta **55**, 3471 (2010).
[26] L. Kosminsky and M. Bertotti, Electroanalysis **11**, 623 (1999).
[27] İ. Çakar, K. V. Özdokur, B. Demir, E. Yavuz, D. O. Demirkol, S. Koçak, S. Timur, and F. N. Ertaş, Sens. Actuat. B **185**, 331 (2013).
[28] S. Cherevko and C. H. Chung, Sens. Actuat. B **142**, 216 (2009).
[29] Y. Ma, J. Di, X. Yan, M. Zhao, Z. Lu, and Y. Tu, Biosens. Bioelectron. **24**, 1480 (2009).
[30] H. X. Wu, W. M. Cao, Y. Li, G. Liu, Y. Wen, H. F. Yang, and S. P. Yang, Electrochim. Acta **55**, 3734 (2010).
[31] W. Wang, Z. Li, W. Zheng, J. Yang, H. Zhang, and C. Wang, Electrochem. Commun. **11**, 1811 (2009).

DOI:10.1063/1674-0068/27/05/600-606